Stabilization regimes and flame structure at the flame base of a swirled lean premixed hydrogen–air injector with a pure hydrogen pilot injection

Justin Bertsch, Thierry Poinsot, Nicolas Bertier, Jiangheng Loïc Ruan

Proceedings of the Combustion Institute 40 (2024) 105660

Contents lists available at ScienceDirect

Proceedings of the Combustion Institute

journal homepage: www.elsevier.com/locate/proci

Stabilization regimes and flame structure at the flame base of a swirled lean premixed hydrogen–air injector with a pure hydrogen pilot injection

Justin Bertsch [a,b,*], Thierry Poinsot [b,c], Nicolas Bertier [a], Jiangheng Loïc Ruan [d]

[a] DMPE, ONERA, Université de Toulouse, 31000 Toulouse, France
[b] Centre Européen de Recherche et de Formation Avancée en Calculs Scientifiques, CERFACS, Toulouse, France
[c] Institut de Mécanique des Fluides de Toulouse, IMFT, Université de Toulouse, CNRS, Toulouse, France
[d] DMPE, ONERA, Université Paris Saclay, 91120 Palaiseau, France

ARTICLE INFO

Keywords:
Combustion
Hydrogen
Swirled
High pressure
CFD

ABSTRACT

Hydrogen (H_2) has become a key in the decarbonation process of the aeronautical field and new gaseous injection systems must be designed to suit hydrogen's specific properties (high laminar flame speed, high adiabatic temperature, large flammability limits and fast diffusivity (Le<1)). In this study, Large Eddy Simulation (LES) and Direct Numerical Simulation (DNS) are performed for a co-axial injector including an annular premixed hydrogen–air, swirled injection surrounding a central axial pure hydrogen lance. LES of the injector installed in a full chamber are performed at 12 bar and the LES resolution issues associated with these high pressures are presented. LES reveals that the flame is stabilized on the rim separating the premixed and the pure hydrogen streams. The stabilization is produced by a structure called RSE for Rim Stabilized Edge Flame. To avoid resolution issues of the LES, the RSE flame structure is analyzed using CANTERA 1D flames and a 2D DNS of the attachment region. Extinction limits are described and implications for flame stability are discussed.

1. Introduction

In a decarbonation context of the gas turbines, hydrogen is an excellent candidate to replace kerosene [1]. However, switching to hydrogen requires new types of injection systems. Specific properties of hydrogen such as high laminar flame speed, high adiabatic flame temperature, large flammability limits and fast diffusivity (Le<1) makes the development of new injectors even more challenging.

Nowadays many injectors and burners specific to hydrogen are developed: HYLON at IMFT Toulouse [2], IHI at ONERA [3], AHEAD at TU Berlin [4], MICROMIX at Aachen University [5] or PPBB at NTNU Trondheim [6]. At the same time at a smaller scale, DNS are also conducted to understand hydrogen flame specificities such as flame turbulence interaction [7,8]. The development of these technologies is costly and Computational Fluid Dynamics (CFD) has become a key tool in the design process or in the prediction of their behavior at high pressure.

The scope of the present work is to use Large Eddy Simulation (LES) on a high pressure injection system to understand the flame topology for tuning purposes.

A crucial issue for LES of H_2 injection systems is accuracy. While kerosene–air computation have been performed and tuned for decades, hydrogen computations at high pressures raise a number of new difficulties. Indeed, hydrogen flames are very thin: premixed flame thicknesses vary as the invert of pressure ($1/P$), which makes the computations of real application at high pressure even more challenging from a numerical point of view. Since kinematic viscosity also decreases like $1/P$, going to high pressure also increases the Reynolds number of the flow leading to additional resolution constraints. Here, computations were performed with the CFD code AVBP, developed at CERFACS and used by many laboratories such as IMFT in Toulouse, EM2C in Centralesupelec, TU Munich, Von Karmann Institute or ETH Zurich and industries such as Safran Aircraft Engines, Safran Helicopter Engines or ArianeGroup. AVBP is used in LES (Section 2) and Direct Numerical Simulation (DNS) modes (Section 5.2)

For CFD of turbulent reacting flow the regime in which combustion proceeds: premixed or diffusion controls the choice of the models. The topology of H_2 flames is an issue in itself, depending often on the details of injection. The present hydrogen injection system is developed in the PHYDROGENE project (Fig. 1) by adapting the existing MICADO injector of ONERA [9,10] which was used for hydrocarbons. The injector has two inlets for hydrogen: H_2 is injected in a central tube, surrounded by a swirled premixed H_2/air gas. Therefore the

* Corresponding author at: DMPE, ONERA, Université de Toulouse, 31000 Toulouse, France.
E-mail address: justin.bertsch@onera.fr (J. Bertsch).

https://doi.org/10.1016/j.proci.2024.105660
Received 27 November 2023; Accepted 10 July 2024
Available online 13 August 2024

flame structure is unknown: premixed as well as diffusion flamelets are expected and they might also interact. Moreover, LES is performed here at 12 bar, making resolution issues more critical. Another specificity is the existence of thermodiffusive instabilities which are still an open issue for lean hydrogen flames [11,12]. At $P = 10$ bar, $T = 700$ K, $\phi = 0.5$ the wrinkling characteristic length is estimated at 0.015 mm [13] which cannot be captured by a typical LES grid of 0.1 mm. Attempts have been made to include such a model in LES [14,15]: here the model proposed by Aniello et al. [16] is used to tackle this issue in the artificially thickened flames framework (TD-TFLES). The TD-TFLES model increases the local reaction rate in very lean premixed flames to model the subgrid-scale wrinkling due to cell formations.

This paper first presents a full LES of the PHYDROGENE injection system, mounted in the MICADO combustion chamber at 12 bar. Section 2 describes the geometry and the numerical setup, while Section 3 presents LES results with several grid refinements up to 220 Mcells. While LES reveals that the flame base is controlled by two coupled flamelets (a lean premixed and a stoichiometric diffusion one), the question of the accuracy is handled in Section 4 to analyze this dual flame structure differently without having to worry about LES resolution. In Section 5 two canonical flame structures are used to elucidate the flame topology observed in the LES (Section 3): a dual flame computed with CANTERA [17] and a Rim Stabilized Edge (RSE) flame is also computed using AVBP in a DNS mode, zooming on the lips of the PHYDROGENE setup. Results confirms that the flame structure revealed by LES is also captured by detailed 1D and 2D simulations. While these results are consistent, they do not prove that LES will always be accurate in this stabilization zone where the meshing requirements are much too stringent to be fulfilled as shown in Section 4 and models (such as TFLES) will always be required.

2. PHYDROGENE injector & numerical set-up

High pressure pre-heated air is injected in the left plane and will be called main injection (Fig. 1). Pure hydrogen is then added in the stream with 8 radial holes with a diameter of 1 mm each (Inj. 1 to 8) before the swirl blades. The back-plane of the chamber is a multi-perforated wall that injects cooling air in the chamber. At the downstream tip of the injector, a 2 mm wide hole injects pure hydrogen, this inlet is called pilot.

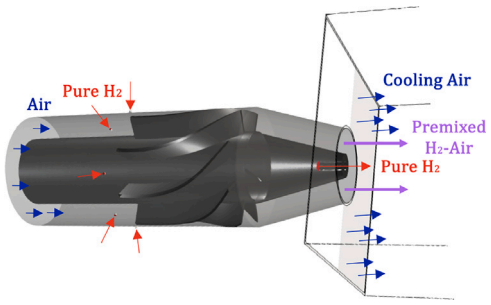

Fig. 1. PHYDROGENE injector — Main air (blue, left) and cooling air (blue, right) injection, fuel injection holes (red, left), pilot injection (red, right). (For interpretation of the references to color in this figure legend, the reader is referred to the web version of this article.)

As a first numerical approach, this technically premixed injection is replaced by a perfectly premixed $H_2 - air$ mixture. The injection holes are not simulated and the hydrogen mass flow is added to the main air injection (Table 1). Numerical boundary conditions are presented in Fig. 2. NSCBC [18] is used for the main (a), pilot (g), cooling inlet (b) and for the chamber outlet (e) as well. Chamber walls (c, d) are considered as iso-thermal walls at $T = 800$ K. Injector lips are iso-thermal walls at $T = 400$ K. All other walls are adiabatic.

Table 1
Inlets properties.

	Main	Pilot	Cooling
$\dot{q}_m$ (g/s)	435	0.530	176
T (K)	750	290	750
Y_{H_2}	0.0110	1	0
Y_{O_2}	0.2305	0	0.233
Y_{N_2}	0.7585	0	0.767
ϕ	0.4	∞	0

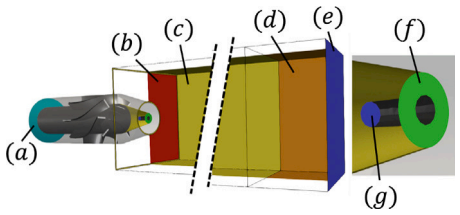

Fig. 2. Numerical boundary conditions: entire domain (left) and zoom on the injector lips (right) — (a) Inlet NSCBC, (b) Inlet NSCBC, (c) Iso-thermal wall $T = 800$ K, (d) Slip iso-thermal wall $T = 800$ K, (e) Outlet NSCBC $P = 12$ bar, (f) Iso-thermal wall $T = 400$ K, (g) Inlet NSCBC.

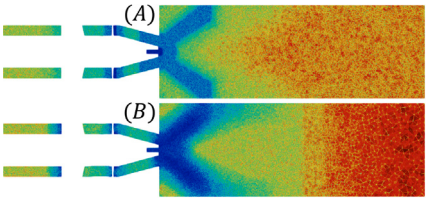

Fig. 3. $+Z$ normal cuts of the computational meshes colored with cell sizes — (A) 96.10^6 elements (geometric refinement), (B) 220.10^6 elements (Static Mesh Refinement using Tekigo and MMG3D).

A cold-flow is first stabilized on a coarse mesh with geometrical refinement zones, then refined before ignition by applying an iso-factor to the cell sizes which leads to Fig. 3A mesh containing 96.10^6 elements. Thanks to the mean results obtained from mesh (A), a mesh (B) containing 220.10^6 elements is built using the mesh refinement tools Tekigo [19] and MMG3D [20] to refine zones based on physical phenomena, measured by metrics fields rather than on geometrical shapes. Two new meshes of 74 and 160.10^6 elements (called 74M and 160M) are generated from the mesh (B) by applying an iso-factor of 1.5 and 1.25 respectively. The Lax–Wendroff convection scheme (2nd order) [21] is used and FE 2Δ scheme for diffusion [22].

The Sigma LES model [23] is used to model sub-grid scale stresses, while chemical kinetics rely on the San Diego mechanism for H_2 [24] that contains 9 species and 21 reactions. Flame/turbulence interaction is modeled using the thickened flame approach [25] with a relaxation sensor [26] and Charlette efficiency function [27] with a constant $\beta = 0.3$. Takeno [28] conditioning is used to identify premixed and diffusion flames and thus thickening regions. Thickening is applied only in the premixed zones.

Here, the diffusivity of H_2 raises a first adaptation : the TFLES model requires an evolution of the local value of the equivalence ratio ϕ. In usual TFLES formulation, ϕ is obtained from the local passive scalar z by $\phi = z(1 - z_{st})/(z_{st}(1 - z))$ where z is computed using the Bilger definition [29]. Using Bilger's definition is not easily compatible with TFLES which require reference flame speeds and thickness upstream

of the reactions zones where no preferential diffusion occurs. This is why we rely on an additional passive scalar [30] leading to monotonic (non-monotonic using Bilger [13]) variations of z and ϕ for H_2 flames.

3. Numerical results and analysis

3.1. Instantaneous results and recirculations zones

Fig. 4 displays a snapshot of the stabilized flow on a 2D cut in the stream-wise direction, for the velocity magnitude, temperature and heat release rate. The flame is anchored on the lip separating the H_2 central duct and the premixed injection (Fig. 4, right). It is stable while the downstream part of the flame is more turbulent, which is confirmed by looking at the downstream part of the velocity magnitude field (left). The most striking result is that two reaction zones can be seen at the flame base (right): the main external premixed branch forms the "V" shape of the flame while a central dome corresponds to the pilot diffusion flame that burns with the remaining air of the main premixed branch.

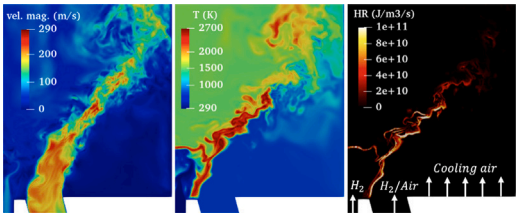

Fig. 4. Half domain, 2D stabilized instantaneous view - 220M mesh.

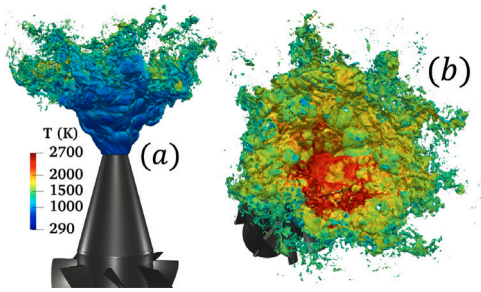

Fig. 5. Instantaneous iso-contour of heat release rate equal to $2e10\,J/m^3/s$ colored by temperature - (a) side view, (b) top view - 220M mesh.

A heat release rate isocontour colored by temperature (Fig. 5) reveals the fluctuating behavior of the flame in the downstream region (Fig. 5a) while the bottom part is stabilized with the high swirling motion. The external part of the flame is under 1500 K (Fig. 5a) while the top view reveals (Fig. 5b) a hot dome in the middle that corresponds to the pilot diffusion flame where temperature is above 2300 K. Recirculation zones are represented with an isocontour of $u = 0\,m\ s^{-1}$ on the mean 3D solution of the 220M mesh averaged over 8 ms, and an isocontour of $T = 1000$ K is also added (Fig. 6). The biggest recirculation zone is internal (IRZ), while two small recirculation zones are observed, CRZ (Corner Recirculation Zone) and ERZ (External Recirculation Zone), located at the cooling plane boundaries. The cooling inlet reduces the temperature in the bottom part of the chamber ($T < 1000$ K) but velocity is not sufficient to suppress the recirculation zone in the four corners of the chamber which leads to pockets of hot gases (ORZ).

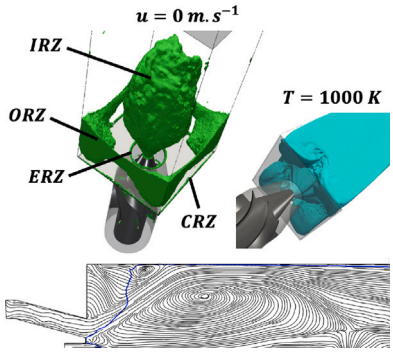

Fig. 6. Recirculation zones visualized by an iso-contour of axial velocity equal to zero ($u = 0\,m\ s^{-1}$) (top left) and stream lines (bottom) - Isocontour of $T = 1000$ K (top right) and blue line (bottom) - 220M mesh. (For interpretation of the references to color in this figure legend, the reader is referred to the web version of this article.)

3.2. Mesh effect on flame topology

Due to the particular topology of the flame at its base where the pilot injection encounters the main premixed injection, an in-depth study of this region is needed because it controls the downstream flow and the overall flame stabilization. Fig. 7 highlights the main characteristics of this particular region. Results are from temporal average of 8 ms and spatial average over 180 planes in the azimuthal direction. The most refined mesh (Fig. 7a) serves as a reference for normalization and comparison.

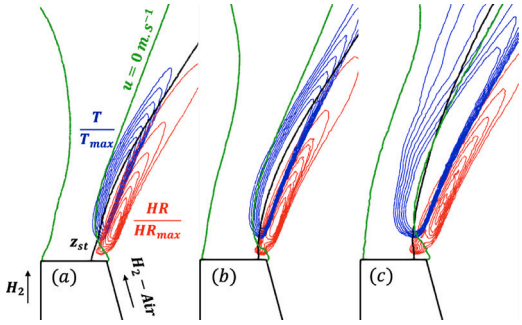

Fig. 7. Isocontour of T/T_{max} varying from 0.9 to 0.975 (blue line), HR/HR_{max} from 0.6 to 0.95 (red line), $u = 0\,m\ s^{-1}$ (green line) and stoichiometric line (black line) on azimuthal means - (a) 220M, (b) 160M, (c) 74M. (For interpretation of the references to color in this figure legend, the reader is referred to the web version of this article.)

Main heat release and temperature zones are encapsulated between the internal recirculation zone (IRZ at $u = 0\,m\ s^{-1}$) and the main swirling flow: the flame position is totally driven by the flow. The maximum heat release rate and temperature zones are not located at the same location: the maximum temperature (blue line) is not at the place where the lean premixed flame burns (red line). It is shifted towards the pure H_2 stream as the premixed flame is lean and is located on the stoichiometric line. In fact, the stoichiometric line divides the high temperature region in two zones: a lean premixed flame and a diffusion flame. The lean premixed reaction creates a first but limited increase of temperature. Then the burnt gases from the lean premixed flame with the remaining air meet the pure hydrogen from the pilot injection and create a pseudo-diffusion flame that elevates the temperature to reach $T_{max} = 2200$ K.

The results on mesh (c) in Fig. 7 seem under resolved but meshes (a) and (b) give essentially uniform results. The flame structure still exhibits a double structure with maximum heat release rate and maximum temperature region close to each other. Thus to retrieve the main characteristics of the flame at a reduced computational cost, mesh (b)

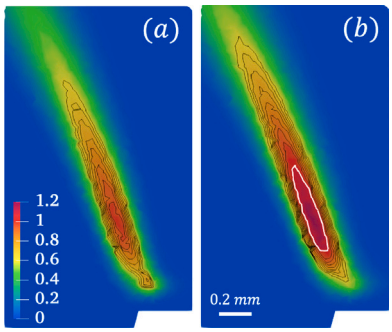

Fig. 8. Normalized azimutal mean (220M mesh) of HR.F with (b) and without (a) TD-TFLES, (a) serves as reference - iso-contours varies from 0.6 to 0.95 - white iso-contour is equal to 1.

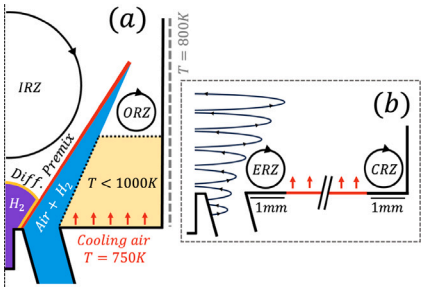

Fig. 9. Proposed flame topology — (a) Global view, (b) Zoom on the chamber bottom.

with 160M cells is sufficient. The TD-TFLES [16] impact on the flame is evaluated in Fig. 8 on the 220M mesh. In the PHYDROGENE LES, the TD-TFLES does not have a significant impact on the heat-release field with a limited increase up to 20%. As its main area of effect is inside the white iso-contour, which is small (≈ 0.4 mm in length), it does not modify the flame structure.

The previous results suggest a global topology for the flame base depicted in Fig. 9. While those results can be used for design, the rest of this paper focuses on one issue: is this LES accurate? To answer this question, resolution issues are first considered in Section 4.

4. Resolution

The LES of Section 3 are performed at 12 bar, $\phi = 0.4$ and $T = 750$ K. At this conditions the thermal thickness of the flame is equal to $\delta_{th} = 0.034$ mm which is more than 13 times smaller than at atmospheric pressure at the same ϕ and T condition ($\delta_{th} = 0.46$ mm).

At atmospheric pressure, $T = 290$ K, the thermal thickness is equal to $\delta_{th} = 0.63$ mm thus the premixed branch can be easily computed and resolved with a grid of $\Delta_x = 0.1$ mm leading to 6.3 points in the flame front. However at 12 bar with a pre-heated air, the flame front is too thin to be fully resolved even with any mesh refinement approach. Knowing this, the previously presented LES results at the flame base must be verified by other means: thus 1D CANTERA flames are used, as well as a 2D DNS limited to the near lip zone. Table 2 summarizes the resolution properties for the 3D LES, 1D CANTERA simulations and a 2D DNS.

A simple indicator of resolution used in Table 2 is $R = \delta_{th}/\Delta_x$. R indicates the number of mesh points used to resolve the inner premixed flame structure. While this indicator does not handle diffusion flame or vorticity zones, it is obviously mandatory to guarantee flame resolution in the PHYDROGENE setup even though it may not be sufficient.

In the 3D LES, R is below unity, confirming that TFLES approach is needed, leading to a thickening factor of approximately 15 to obtain 5 points in the flame front. On the other side, in CANTERA simulations and the 2D DNS of Section 5.2, higher resolutions can be achieved to fully resolve the flame front without models. To be able to achieve the DNS, pressure is brought back to atmospheric pressure and the configuration is two-dimensional so that resolution issues can be solved (at 12 bar cells of 3.4 µm are required to obtain $R = 10$). CANTERA and DNS are now used to understand the flame base topology to provide a reference topology for the LES.

Table 2
Resolution index R for 3D LES (Section 3), 1D CANTERA (Section 5.1) and 2D DNS (Section 5.2)

	$3D\ LES$	$1D\ CAN.$	$2D\ DNS$
P (bar)	12	12	1.01325
T (K)	750	750	290
ϕ	0.4	0.4	0.4
δ_{th} (mm)	0.034	0.034	0.63
Δ_x (mm)	0.1	5.10^{-5}	0.03
$R = \delta_{th}/\Delta_x$	0.34	> 600	21

5. The RSE flame: lean premixed against pure fuel

5.1. Dual 1D flames in CANTERA

Rich methane-air mixture against oxidizer have already been investigated in a stagnation plane which leads to a flame structure similar to the one observed in the LES [31] of Section 3: a first rich premixed flame, followed by a diffusion flame that burns with the remaining fuel in the burnt gases. We will call it a dual flame. This dual structure is not a new configuration: for example, Hamins et al. [32] studied the structure and extinction of a partially premixed, diffusion flame stabilized between a vaporizing surface of heptane and a gaseous stream of CH_4, O_2, and N_2. They observed a dual structure, including a premixed flame close to a diffusion flame. This structure is not yet a RSE flame because it is adiabatic and does not include heat losses to the rim wall, which is important for the RSE flame.

Dual flames in the PHYDROGENE conditions were reproduced (pure fuel against lean premixed gases) in CANTERA [17] at $P = 1$ bar and 12 bar for a wide range of global strains, defined as follow [33],

$$A = \frac{2u_0}{H}\left[1 + \frac{u_f\sqrt{\rho_f}}{u_o\sqrt{\rho_o}}\right] \quad (1)$$

with H the width of the domain, u the velocity, and ρ the volumetric mass while f and o denotes the fuel and oxidizer. Pure H_2 is considered as the fuel. The premixed mixture is set at $T = 750$ K and $\phi = 0.4$ while pure hydrogen is set at $T = 290$ K (same conditions as the 3D LES). Fig. 10 presents the hydrogen source terms for the computed flames with a strain range varying from $A = 4000\,s^{-1}$ to $430\,000\,s^{-1}$. Pure hydrogen is coming from $x_{norm} = 0.3$ while premixed mixture from $x_{norm} = 0.6$ side.

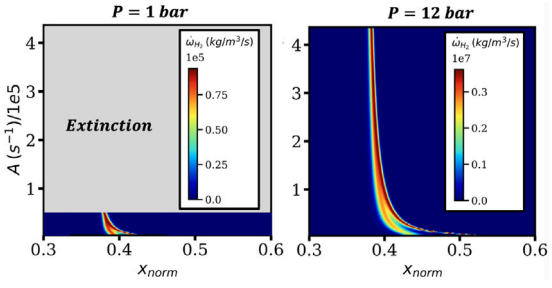

Fig. 10. Scatter plots of H_2 source term of 1D dual flame for multiples strains: $P = 1$ bar, 20 mm domain (left) - $P = 12$ bar, 2 mm domain (right).

At 12 bar (Fig. 10, right) for strain values under $100\,000\,s^{-1}$ (Fig. 11) the lean premixed mixture burns as a classical premixed flame F_p

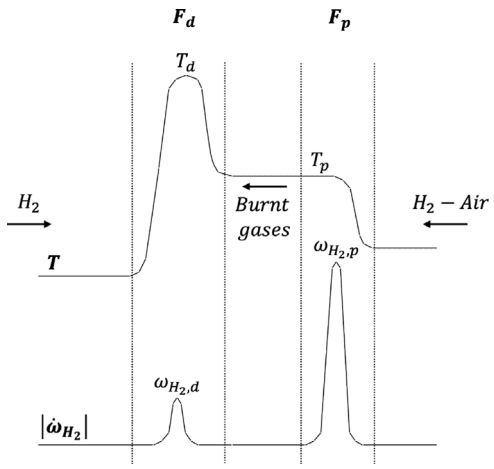

Fig. 11. Illustration of the topology of a dual flame (for $A < 100\,000\,s^{-1}$ at 12 bar and $A < 51\,000\,s^{-1}$ at 1 bar): lean premixed against pure fuel - Temperature (top) and hydrogen source term (bottom).

and creates a first hydrogen consumption peak $\omega_{H_2,p}$ leading to a temperature plateau T_p. Burnt gases produced by F_p are then used as an oxidizer for the H_2 fueled diffusion flame F_d. F_d creates another smaller hydrogen consumption peak $\omega_{H_2,d}$ leading to the maximum temperature T_d.

At higher strains ($A > 100\,000\,s^{-1}$, Fig. 10, right) the dual structure merges as one global temperature/hydrogen source term peak as observed by Hamins et al. [32]. Here, a reduction of the maximum temperature is observed but the temperature remains over 2000 K. No extinction phenomena has been captured even at $A = 430\,000\,s^{-1}$. At atmospheric pressure (Fig. 10, left) the same dual flame is observed, however when the two branches merges at $A \approx 51\,000\,s^{-1}$ extinction appears.

CANTERA can be used to understand the topology of the dual flame away from the lips but cannot predict the lifting or anchoring of the RSE flame. Multiple theories have been proposed to predict the lift-off of diffusion flames [34–36] but none of them have been proven to apply to Rim Stabilized Edge (RSE) flame since the flame structure is different. Even the CANTERA simulation is insufficient because it does not include flow and thermal effects at the cold lips of the injector. Since dual flame also exists at 1 bar a DNS is performed at atmospheric pressure in Section 5.2 to fully describe the RSE flame where all mechanisms are included in a limited size, simplified geometry.

5.2. 2D DNS of a RSE flame

A 2D DNS is computed in a domain of 50 mm by 51 mm with a step of 3 mm wide (same size as PHYDROGENE lips) and 1 mm long at the bottom of the computational domain (Fig. 12).

On the bottom-left side, pure hydrogen is injected while on the bottom-right side, a premixed $H_2 - Air$ mixture at $\phi = 0.4$ is injected. Temperature of both inlets is set at $T = 290$ K and pressure to 1.01325 bar. The velocities are, $u_{H_2,max} \approx 100\,m\,s^{-1}$ and $u_{\phi,max} \approx 45\,m\,s^{-1}$ which represents reasonable speeds for this type of injection system. The step which represents the injector lips is an isothermal wall at $T = 290$ K. A slip boundary condition is used to mimic the far field, represented here by the left and right walls. Cell sizes varies from 0.03 mm in the center of the domain (flame region) to 0.5 mm in the far field, leading to a resolution of 21 points in the flame front (Table 2) which is twice more than usual values.

Fig. 13 presents instantaneous views (cropped domain) of the hydrogen source term for multiple equivalence ratios on the premixed side and with hydrogen on the pilot injection (top) and with nitrogen on the pilot injection (bottom).

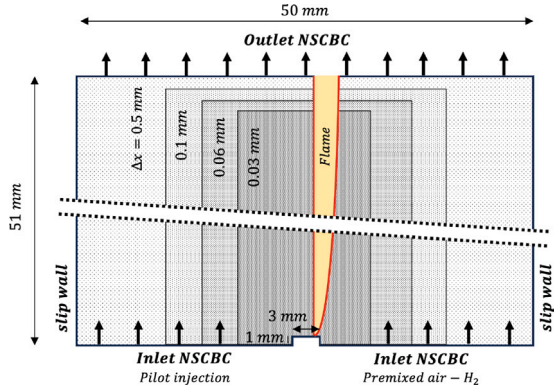

Fig. 12. DNS numerical setup.

The mixture fraction z (Eq. (2)), is used to plot the stoichiometric line ($z = z_{st}$) represented in white.

$$z = \frac{(sY_F - Y_O) - (sY_{F,2} - Y_{O,2})}{sY_{F,1} - Y_{O,1} - (sY_{F,2} - Y_{O,2})} \tag{2}$$

$$z_{st} = \frac{1}{1 + \frac{sY_{F,1}}{Y_{O,2} - sY_{F,2}}} \tag{3}$$

where F indicates fuel (H_2) and O oxidizer (O_2) streams, while index 1 is the pure fuel stream and 2 is the premixed stream. In our case $Y_{O,1}$ is equal to zero and $Y_{F,2}$ is not and depends on the case as well as $Y_{O,2}$. s is the stoichiometric ratio.

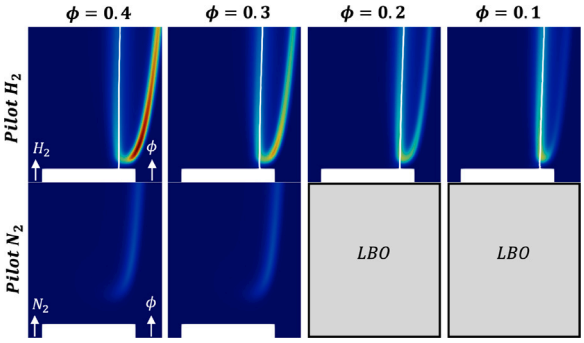

Fig. 13. Instantaneous views of the hydrogen source term for equivalence ratio of the premixed side varying from $\phi = 0.4$ to 0.1 (columns) with H_2 as pilot injection (top) and N_2 (bottom) - Stoichiometric line (white).

These flames almost do not move so that their steady structure can be directly analyzed and no intrinsic flame instability is observed. With hydrogen in the pilot injection (Fig. 13, top), the decrease of the equivalence ratio of the premixed stream leads to an intensity reduction of the premixed branch (right), so that the burnt gases used as the oxidizer for the diffusion branch (left) contain more O_2 which enhances its intensity.

The same flame is computed at 12 bar with a pre-heated mixture ($T = 750$ K) and $\phi = 0.4$ with a mesh size of 5 μm leading to $R \approx 7$ (Fig. 14). The same flame structure is obtained at the lip at high pressure, making the 1 bar case valid for a parametrical study.

To understand the role of the H_2 pure injection, this stream is replaced by N_2 (at 290 K), using the same velocity. This is an arbitrary choice which increases the flow rate of the left stream of the N_2 compared to the H_2 case. However we checked that it plays a limited role. As expected, without H_2 as a pilot injection the RSE structure disappears (Fig. 13, bottom) and a classical premixed flame is obtained.

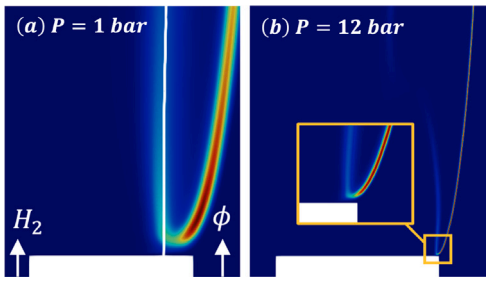

Fig. 14. Hydrogen source term of RSE flame at (a) $P = 1\,\text{bar}$, $T_{H_2,\phi} = 290\,\text{K}$, $\Delta x_{mesh} = 30\,\mu\text{m}$ and (b) $P = 12\,\text{bar}$, $T_{H_2} = 290\,\text{K}$, $T_\phi = 750\,\text{K}$, $\Delta x_{mesh} = 5\,\mu\text{m}$, with a lip size of 3 mm, premixed mixture at $\phi = 0.4$.

At an equivalence ratio $\phi \leq 0.2$ a lean blow off (LBO) is observed, showing that the pure H_2 injection is effective at pushing LBO to lower values.

In conclusion, DNS show that, at every equivalence ratio studied with H_2 as pilot injection, the premixed branch strongly interacts with the diffusion branch. This interaction helps to stabilize the premixed branch at an equivalence ratio equal or below $\phi = 0.2$. This interaction needs to be further studied, for example for hot walls to determine which branch really controls the stabilization process.

An important factor controlling the RSE flame is the heat loss by the flame to the cold lip. This impact can be measured by comparing the local temperature T to the equilibrium temperature T_{eq} which can be evaluated with CANTERA. To ensure a proper comparison of T_{eq} with T in the premixed zone, the local equilibrium temperature (T_{eq}) is conditioned using the progress variable based on H_2O mass fraction [37] such as, $T_{cor} = T_{eq}.c + T_u(1-c)$, with $c = Y_{H_2O}/Y_{H_2O,burnt}$ and T_u being the fresh gases temperature. Fig. 15 presents the hydrogen source term for the RSE flame at $\phi = 0.4$ from Fig. 13 with contours of temperature (T) minus local corrected equilibrium temperature (T_{cor}).

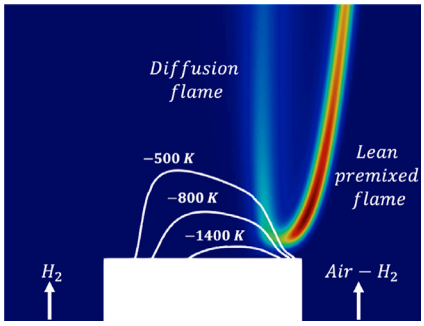

Fig. 15. Hydrogen source term for RSE flame at $\phi = 0.4$ with contours of $T - T_{cor}$ equal to −500, −800 and −1400 K.

Diffusion and lean premixed branch merge into one point called the double point, which is stabilized in the Cold Rim Thermal Zone (CRTZ) where more than 1400 K are lost compared to the corrected equilibrium value T_{cor}: in this zone the structure of the RSE flame is strongly controlled by the heat losses to the cold rim and it does not move anymore. It is not a standard propagating adiabatic edge flame.

These DNS results allow us to propose a conceptual model for RSE flames shown in Fig. 16.

This flame is close to a triple flame [38] without the rich premixed branch. However, while triple flames propagate at a speed larger than the premixed flame speeds, the RSE flame stops propagating when it reaches the cold zone near the rim. This type of edge flames obviously requires more studies to analyze its structure and resistance to flow and heat constraints.

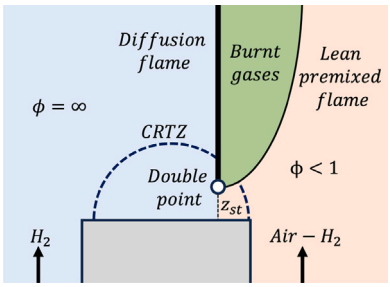

Fig. 16. Conceptual model for a RSE (Rim Stabilized Edge) flame formed when the pure H_2 injection stream meets the premixed $air - H_2$ stream.

6. Conclusion

The stabilization of a pure H_2 versus premixed H_2-air flame has been successfully simulated using the CFD code AVBP at high pressure ($P = 12\,\text{bar}$) in LES mode, revealing that the flame base was controlled by a dual premixed/diffusion structure.

A priori resolution criteria show that even if the LES achieved mesh convergence, resolution was too low to fully rely on the LES data so that the structure of this flame was then investigated during 1D simulations and DNS of 2D RSE flames with much higher resolutions.

CANTERA counterflow flames simulations confirm the dual flame structure and reveal that even at a high level of global strain (up to $A = 100000\,\text{s}^{-1}$ at 12 bar) a double structure is obtained. Since CANTERA cannot account for heat transfer to the lip and flow effects, a 2D DNS was also performed to understand the flame topology at its attachment point near the lips leading to a RSE flame. The RSE flame obtained in the DNS exhibits two branches like a dual flame but merges at a double point where the diffusion and the lean premixed branch merge as one near the lip. At very lean conditions ($\phi \leq 0.2$) the premixed flame cannot be stabilized without the H_2 pilot injection, confirming that the RSE flame structure helps stabilize lean premixed flames.

Future works will focus on a Coupled Heat Transfer (CHT) approach to determine the injector's lips and chamber wall temperatures which can impact the topology of the flame by modifying recirculation zones [39] and the double point location at the injector's lips which can dramatically change the flame topology.

Novelty and significance statement

The paper describes how a hydrogen flame produced on a coaxial injector (pure hydrogen next to hydrogen/air mixture) stabilizes on a cold lip, through a structure called here a Rim Stabilized Edge Flame (RSE). The RSE flame is studied at high pressure using LES and CANTERA 1D simulations and at atmospheric pressure using DNS. It combines a diffusion and a premixed flame stabilized by the heat losses to the lip.

CRediT authorship contribution statement

Justin Bertsch: Wrote the paper, Performed research, Analyzed data. **Thierry Poinsot:** Designed research, Reviewed the paper. **Nicolas Bertier:** Designed research, Reviewed the paper. **Jiangheng Loïc Ruan:** Designed research, Reviewed the paper.

Declaration of competing interest

The authors declare that they have no known competing financial interests or personal relationships that could have appeared to influence the work reported in this paper.

Acknowledgments

This work was funded by the French Government (DGAC, French Civil Aviation Authority) as part of the PHYDROGENE project (“France 2030” plan).

References

[1] European Union, Fuel Cells and Hydrogen 2 Joint Undertaking, Hydrogen-powered aviation – A fact-based study of hydrogen technology, economics, and climate impact by 2050, Publications Office, 2020.
[2] A. Aniello, D. Laera, S. Marragou, H. Magnes, L. Selle, T. Schuller, T. Poinsot, Experimental and numerical investigation of two flame stabilization regimes observed in a dual swirl H2-air coaxial injector, Combust. Flame 249 (2023) 112595.
[3] J.L. Ruan, A. Vincent-Randonnier, G. Pilla, C. Irimiea, Development of innovative low NOx hydrogen-fueled burner for aeronautic applications, in: Turbo Expo: Power for Land, Sea, and Air, Vol. 3A: Combustion, Fuels, and Emissions, 2023, V03AT04A001.
[4] T.G. Reichel, K. Goeckeler, O. Paschereit, Investigation of lean premixed swirl-stabilized hydrogen burner with axial air injection using OH-PLIF imaging, J. Eng. Gas Turbines Power 137 (11) (2015) 111513.
[5] H.H.-W. Funke, S. Boerner, J. Keinz, K. Kusterer, D. Kroniger, J. Kitajima, M. Kazari, A. Horikawa, Numerical and experimental characterization of low NOx micromix combustion principle for industrial hydrogen gas turbine applications, in: Turbo Expo: Power for Land, Sea, and Air, Vol. 2A and B: Combustion, Fuels and Emissions, 2012, pp. 1069–1079.
[6] C. Meraner, T. Li, M. Ditaranto, T. Løvås, Combustion and NOx emission characteristics of a bluff body hydrogen burner, Energy Fuels 33 (2019) 4598–4610.
[7] A.J. Aspden, M.S. Day, J.B. Bell, Turbulence-flame interactions in lean premixed hydrogen: Transition to the distributed burning regime, J. Fluid Mech. 680 (2011) 287–320.
[8] M. Rieth, A. Gruber, F.A. Williams, J.H. Chen, Enhanced burning rates in hydrogen-enriched turbulent premixed flames by diffusion of molecular and atomic hydrogen, Combust. Flame 239 (2022).
[9] A. Cochet, V. Bodoc, C. Brossard, O. Dessornes, C. Guin, R. Lecourt, M. Orain, A. Vincent-Randonnier, ONERA test facilities for combustion in aero gas turbine engines, and associated optical diagnostics, Aerosp. Lab Issue 11-June 2016 (11) (2016).
[10] C. Irimiea, A. Vincent-Randonnier, J.P. Dufitumukiza, S. Puggelli, J.-B. May-Carle, et al., ALTERNATE: Experimental and modeling study of soot formation in high-pressure kerosene and SAF combustion, in: Towards Sustainable Aviation Summit 2022 (TSAS 2022), Toulouse, France.
[11] P.E. Lapenna, L. Berger, A. Attili, R. Lamioni, N. Fogla, H. Pitsch, F. Creta, Data-driven subfilter modelling of thermo-diffusively unstable hydrogen–air premixed flames, Combust. Theory Model. 25 (2021) 1064–1085.
[12] P.E. Lapenna, A. Remiddi, D. Molinaro, G. Indelicato, F. Creta, A-posteriori analysis of a data-driven filtered wrinkled flamelet model for thermodiffusively unstable premixed flames, Combust. Flame 259 (2024).
[13] L. Berger, A. Attili, H. Pitsch, Intrinsic instabilities in premixed hydrogen flames: Parametric variation of pressure, equivalence ratio, and temperature. Part 1 - dispersion relations in the linear regime, Combust. Flame 240 (2022) 111935.
[14] V. Molkov, D. Makarov, A. Grigorash, Cellular structure of explosion flames: Modeling and large-eddy simulation, 176, Taylor and Francis Inc., 2004, pp. 851–865,
[15] R. Keppeler, M. Pfitzner, Modelling of Landau–Darrieus and thermo-diffusive instability effects for CFD simulations of laminar and turbulent premixed combustion, Combust. Theory Model. 19 (2015) 1–28.
[16] A. Aniello, D. Laera, L. Berger, A. Attili, T. Poinsot, Introducing thermodiffusive effects in large Eddy simulation of turbulent combustion for lean hydrogen-air flames, in: Proceedings of the 2022 Summer Program, Stanford, NASA, 2022.
[17] D. Goodwin, H. Moffat, I. Schoegl, R. Speth, B. Weber, Cantera: An object-oriented software toolkit for chemical kinetics, thermodynamics, and transport processes, 2023, Version 3.0.0.
[18] T. Poinsot, S. Lele, Boundary conditions for direct simulations of compressible viscous flows, J. Comput. Phys. 101 (1992) 104–129.
[19] COOP Team CERFACS, Tekigo, available (Dec. 2023) at http://opentea.pg.cerfacs.fr/tekigo/.
[20] C. Dobrzynski, MMG3D: User guide, Technical Report, (RT-0422) INRIA, 2012.
[21] P.D. Lax, B. Wendroff, Systems of conservation laws, Comm. Pure Appl. Math. 13 (1960) 217–237.
[22] O. Colin, M. Rudgyard, Development of high-order Taylor-Galerkin schemes for LES, J. Comput. Phys. (2000) 338–371.
[23] F. Nicoud, H.B. Toda, O. Cabrit, S. Bose, J. Lee, Using singular values to build a subgrid-scale model for large eddy simulations, Phys. Fluids 23 (8) (2011) 085106.
[24] P. Saxena, F.A. Williams, Testing a small detailed chemical-kinetic mechanism for the combustion of hydrogen and carbon monoxide, Combust. Flame 145 (2006) 316–323.
[25] T. Butler, P. O’Rourke, A numerical method for two dimensional unsteady reacting flows, Symp. Combust. 16 (1) (1977) 1503–1515.
[26] T. Jaravel, Prediction of Pollutants in Gas Turbines Using Large Eddy Simulation (Ph.D. thesis), Université de Toulouse, France, 2016.
[27] F. Charlette, C. Meneveau, D. Veynante, A power-law flame wrinkling model for LES of premixed turbulent combustion part I: non-dynamic formulation and initial tests, Combust. Flame 131 (1–2) (2002) 159–180.
[28] H. Yamashita, M. Shimada, T. Takeno, A numerical study on flame stability at the transition point of jet diffusion flames, Symp. Combust. 26 (1) (1996) 27–34.
[29] R. Bilger, S. Stårner, R. Kee, On reduced mechanisms for methane air combustion in nonpremixed flames, Combust. Flame 80 (2) (1990) 135–149.
[30] H.J. Vargas Ruiz, D. Laera, G. Lartigue, L. Gicquel, Thickened flame model for multi-fuel multi-injection combustion, in: 46th Meeting of the Italian Section of the Combustion Institute, Italian section of the combustion institute, Bari, Italy, 2024.
[31] B. Fiorina, O. Gicquel, L. Vervisch, S. Carpentier, N. Darabiha, Approximating the chemical structure of partially premixed and diffusion counterflow flames using FPI flamelet tabulation, Combust. Flame 140 (2005) 147–160.
[32] A. Hamins, H. Thridandam, K. Seshadri, Structure and extinction of a counterflow partially premixed, diffusion flame, Chem. Eng. Sci. 40 (11) (1985) 2027–2038.
[33] U. Niemann, K. Seshadri, F.A. Williams, Accuracies of laminar counterflow flame experiments, Combust. Flame 162 (2015) 1540–1549.
[34] L. Muñiz, M. Mungal, Instantaneous flame-stabilization velocities in lifted-jet diffusion flames, Combust. Flame 111 (1) (1997) 16–31.
[35] T.F. Guiberti, W.R. Boyette, Y. Krishna, W.L. Roberts, A.R. Masri, G. Magnotti, Assessment of the stabilization mechanisms of turbulent lifted jet flames at elevated pressure using combined 2-D diagnostics, Combust. Flame 214 (2020) 323–335.
[36] S. Marragou, H. Magnes, A. Aniello, T. Guiberti, L. Selle, T. Poinsot, T. Schuller, Modeling of H2/air flame stabilization regime above coaxial dual swirl injectors, Combust. Flame 255 (2023) 112908.
[37] L. Berger, A. Attili, H. Pitsch, Intrinsic instabilities in premixed hydrogen flames: parametric variation of pressure, equivalence ratio, and temperature. Part 2 – Non-linear regime and flame speed enhancement, Combust. Flame 240 (2022) 111936.
[38] D. Veynante, L. Vervisch, T. Poinsot, A. Liñán Martínez, G. Ruetsch, Triple flame structure and diffusion flame stabilization, in: Studying Turbulence using Numerical Simulation Databases. V : Proceedings of the 1994 Summer Program, Stanford University, Stanford, 1995.
[39] P. Benard, G. Lartigue, V. Moureau, R. Mercier, Large-eddy simulation of the lean-premixed PRECCINSTA burner with wall heat loss, Proc. Combust. Inst. 37 (4) (2019) 5233–5243.